Mapana – Journal of Sciences
2026, Vol. 25, No. 1, *49-71*
ISSN 0975-3303 | https://doi.org/10.12723/mjs.76.4

Experimental and Computational Studies on Coumarin 4-(4-Methoxy-Phenoxymethyl)-6-Phenyl-Chromen-2-one and Estimation of Ground-State and Singlet Excited-State Dipole Moments by Solvatochromic Approach

Alageri Lingappa*, Shivaleela Basavaraj*, Srinath*, Kuncham Narasimhulu†, Thipperudrappa J‡, S. M. Hanagodimath*

Abstract

The absorption and emission properties of coumarin-4-(4-Methoxy-Phenoxymethyl)-6-phenyl-chromen-2-one **(4MPPC)** at room temperature are investigated in pure polar and nonpolar solvents. The pure solvents influence on spectral characteristics. This is investigated by applying theories such as the Lippert-Mataga polarity function, Reichardt's microscopic solvent polarity parameter, and Kamlet and Catalan's multiple linear regression techniques. The main role of solute and solvent interaction in pure solvents, particularly, depends on dielectric properties and hydrogen bonding. The computed HOMO and LUMO energies of the compound indicate that they are chemically active with a tendency for molecular interactions and are supported by the electrostatic potential data. The electric dipole moments of both the ground and excited states have been estimated using the solvatochromic shift method. The value of the electric dipole moment of the excited state and the redshifts of emission spectra show that the emitting single state has an intramolecular charge transfer character (ICT). From the present work, we conclude that both polar and nonpolar solvents change the fluorescent properties of coumarin.

* Department of PG Studies and Research in Physics, Gulbarga University, Kalaburagi, Karnataka, India; alagerilingappa@gmail.com, smhmath@rediffmail.com

† Department of Physics, SSA Govt. First Grade College (Autonomous), Ballari, Karnataka, India; drsimhasku@gmail.com

‡ Department of Physics, Vijayanagara Sri Krishnadevaraya University, Ballari, Karnataka, India

Keywords: Density Functional Theory, Optimized Vector, LUMO, HOMO, Molecular electrostatic potential surface, absorption, fluorescence spectra, UV-VIS spectrum, IR spectra, Dipole moments and Polarizability.

1. Introduction

The study of the effect of solvents on the absorption and fluorescence properties of organic fluorophores has been an interesting investigation for many years. These investigations have considerable importance in the field of photophysics and photochemistry [1-2]. The experimental and computational methods are very important for the determination of ground and excited state dipole moments and investigations of photophysical properties like fluorescence quantum yield(Φf), fluorescence lifetime (τ_f), absorption and fluorescence spectral shift, etc. The knowledge of the excited state dipole moments of electronically excited molecules is quite useful in designing nonlinear optical materials [3]. Differential stabilization of ground and excited states are observed when the polarities of the solvents are varied [4]. Solvatochromism is the most commonly established method due to its high linear correlation between solvent polarity functions and spectroscopic parameters. The solvatochromic shift method has been adopted to determine the ground and excited state dipole moments of various fluorescent molecules, including coumarins [5]. The present investigation focuses on the estimation of ground and excited state dipole moments of coumarin **4MPPC molecule** using solvents with different polarities [5].

The solvatochromic characteristics of coumarin 4MPPC have been investigated using Kamlet's and Catalan's solvent polarity parameters to understand specific and non-specific interactions between the solute and solvents [6]. In fact, to the best of our knowledge, there have been no reports on the determination of ground and excited state dipole moment values of **4MPPC** [6].

The molecule **4MPPC** is a coumarin (chromen-2-one) derivative containing multiple aromatic rings and heteroatoms, because of its extended π – conjugation, substituent effects, and possible intramolecular interactions. Density Functional Theory (DFT) is an appropriate method to study its optimized geometry and electronic structure.

2. DFT Structure of 4MPPC

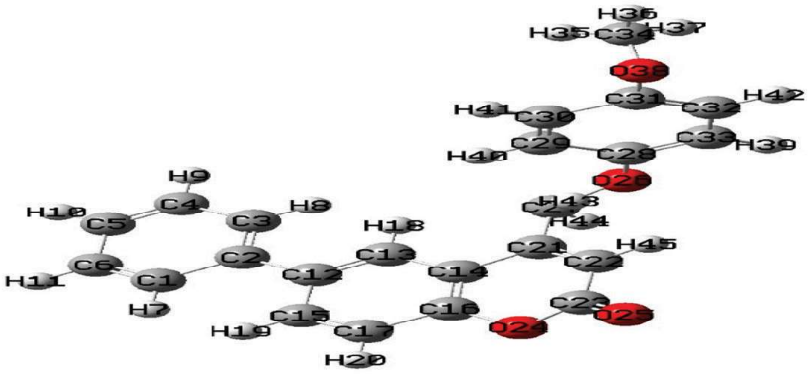

Figure 1: DFT Structure of 4MPPC

3. Optimized Vector (OPT-Vector) of 4MPPC

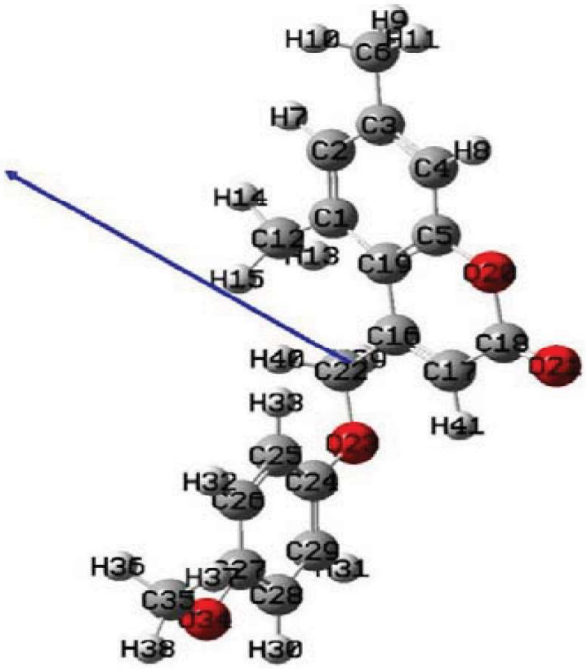

Figure 2: OPT Vector of 4MPPC

4. Electrostatic potential surface

Electrostatic potential is created by the molecule's electron distribution and atomic nuclei. The three-dimensional charge distributions of molecules are depicted by the electrostatic potential surfaces [7-8]. It is used to understand how molecules interact and optimize their electrostatic complementary [8]. It shows regions of positive and negative electrostatic potential around a molecule. ESP is a computational method that uses artificial intelligence to

predict the properties of molecules [9]. If the discussion is about molecular properties or molecular interactions, it likely refers to the electrostatic potential. If the discussion is about computational methods for predicting chemical behaviour, it could be an Electrostatic potential surface [9-10].

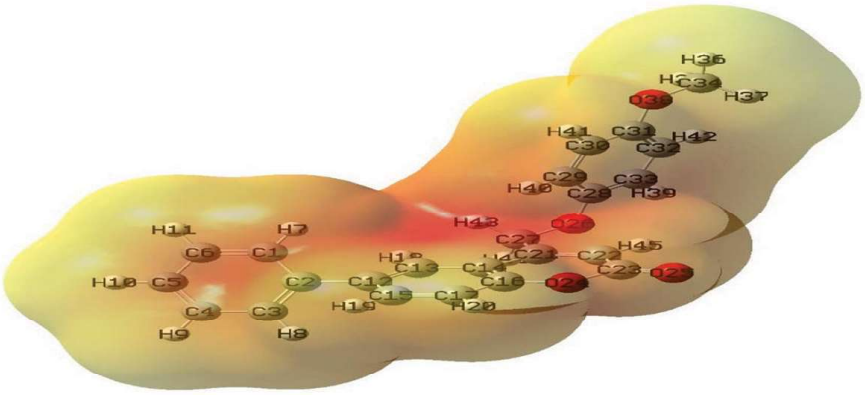

Figure 3: EPS of 4MPPC

The molecular electrostatic potential surface of coumarin 4MPPC was generated using Gaussian 16W software with B3LYP/6-31 basis set, as shown in the fig.3. The surface plot reveals that electrophilic regions are predominantly located around O_2, indicating that O_2 acts as an electron donor in the compound [11-12]. The positive regions, which are nucleophilic and act as acceptors, are located over the CH_4 group. This uneven charge distribution leads to a higher dipole moment [12-13]. The molecular electrostatic potential helps identify sites for electrophilic attack, nucleophilic reactions, and hydrogen bonding interactions [14].

5. Main Insights

The 4MPPC is a highly conjugated coumarin derivative with environment-sensitive fluorescence and strong nonlinear optical properties, featuring characteristic IR and UV-Vis absorption features that reflect its extended π-system and functionalized scaffold [15-16]. Its photo-physical and spectroscopic properties make it a candidate for optoelectronics, sensors, and bioimaging [17-18].

6. Core Molecular Features

- Formula: $C_{23}H_{18}O_4$.
- Exact Mass: 358 amu.
- Molar Mass: 358g mol^{-1}.

Double Bond Equivalents (DBE): 15 (high aromaticity and conjugation). LogP: ~4.0-4.6 (hydrophobic, organic soluble) [18].

Topology: Lactone (chromen-2-one core) + 6-phenyl + methoxy-phenoxy methyl (electron-donating substituent) [19].

7. Photophysical Properties

Absorption and Emission

UV-VIS Absorption: Dominant π–π* band typically 320–380 nm, with the maximum (λ_{max}) shifting to the higher 300 nm due to the electron-donating substituents and extended conjugation [19-20].Emission: Blue-green region (400–520 nm), with emission red-shifting in polar solvents; the Stokes shift is moderate (60–140 nm).Quantum Yield (Φ_f): Predicted 0.3–0.8; higher in non-protic, rigid media and lower with H-bonding or quenching processes [21-22]. Lifetime (τ_f): ~1–5 ns in air-saturated solution; longer in deoxygenated/ nonpolar Environments [23].

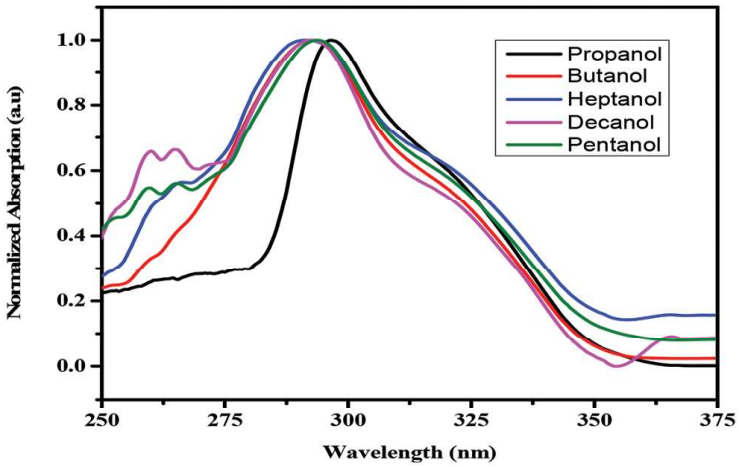

Figure 4: Absorption spectra of 4MPPC in polar solvents

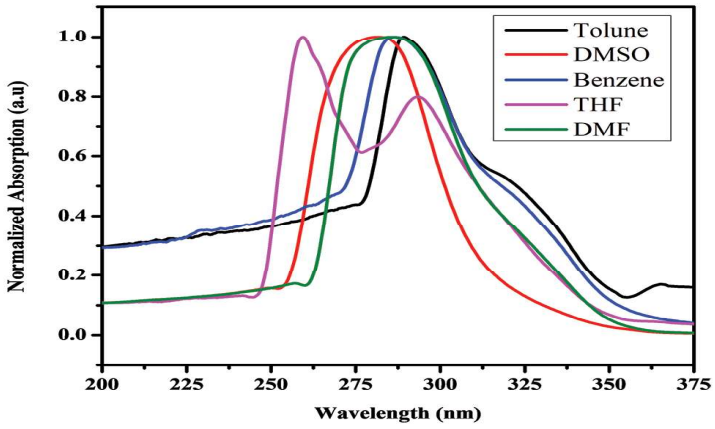

Figure 5: Absorption spectra of 4MPPC in nonpolar solvents

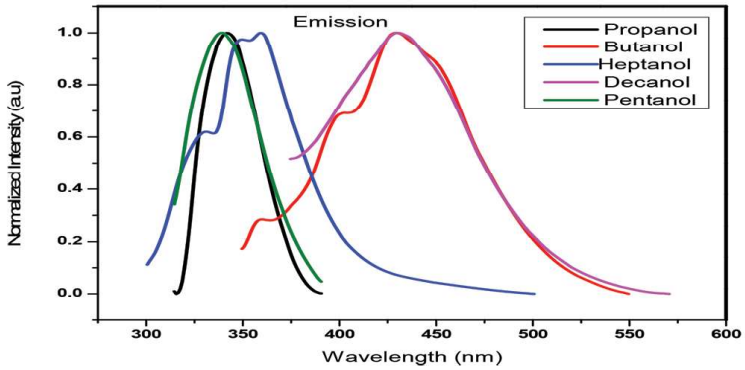

Figure 6: Fluorescence spectra of 4MPPC in polar solvents

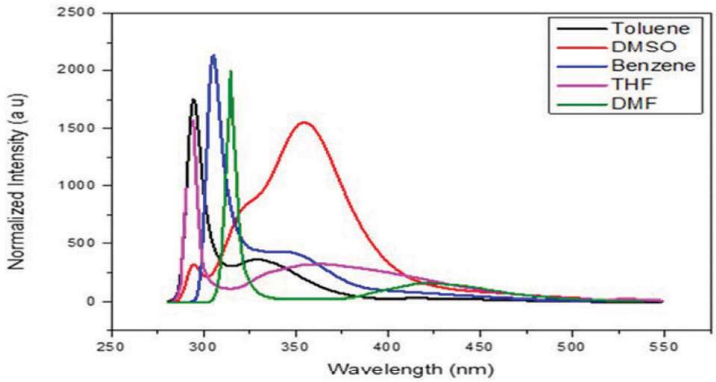

Figure 7: Fluorescence spectra of 4MPPC in nonpolar solvents

7.1. Effect of solvents on absorption and fluorescence spectra of coumarin 4MPPC

The absorption and fluorescence spectra of the coumarin molecule 4MPPC were recorded in various solvents with increasing polarity at room temperature [24]. Absorption and fluorescence maximum wavelength of coumarin **4MPPC** [24-25], was found to be in the range of 258–298 nm and 339–434 nm, respectively, in the chosen solvents [25-26]. Absorption maxima ($\bar{\nu}_a$), emission maxima ($\bar{\nu}_f$), Stokes shifts ($\bar{\nu}_a - \bar{\nu}_f$) and the arithmetic mean of Stokes shift values (in cm^{-1}) were calculated and tabulated [26].

8. Equations for the estimation of dipole moments

The independent equations used for the estimation of ground and excited state dipole moments in various solvents with varied dielectric constant (ε) and refractive index (n) are as follows,

Lippert-Mataga equation- $\bar{\nu}_a - \bar{\nu}_f = m_1 f_1(\varepsilon\, n) + Constant$

Bakhshiev's equation - $\bar{\nu}_a - \bar{\nu}_f = m_2 f_2(\varepsilon\, n) + Constant$

Kawski-Chamma-Viallet's equation [27]

$$\frac{\bar{\nu}_a + \bar{\nu}_f}{2} = -m_3 f_4(\varepsilon\, n) + Constant$$

Where $\bar{\nu}_a$ and $\bar{\nu}_f$ are absorption and emission maxima wave numbers in cm^{-1}

8.1. Estimation of excited-state dipole moments

The dipole moment of coumarin (4MPPC) was calculated using Bakshiev's and Kawski-Chamma-Viallet's equations [28]. Using these polarity parameters, the following expressions can be obtained to estimate μ_e and μ_g

$$\mu_g = \frac{m_2 - m_1}{2}\left(\frac{hca^3}{2m_1}\right)^{1/2} \quad \mu_g = \frac{m_2 + m_1}{2}\left(\frac{hca^3}{2m_1}\right)^{1/2}$$

The slopes m_1 and m_2 are obtained from the plots of $(\bar{\nu}_a - \bar{\nu}_f)$ versus $f_1(\varepsilon\, n)$, and $\frac{(\bar{\nu}_a + \bar{\nu}_f)}{2}$ versus $f_2(\varepsilon\, n)$ for different solvents, respectively [28-29].

Where **h** is Planck's constant, a is the Onsager cavity radius of a molecule, and c is the velocity of light [29].

If μ_e and μ_g are not parallel to one another, then the angle ϕ between μ_e and μ_g can be estimated using the below

$$\cos \emptyset = \frac{1}{2\mu_g \mu_e}\left[\left(\mu_g{}^2 + \mu_e{}^2\right) - \frac{m_2}{m_1}\left(\mu_e{}^2 - \mu_g{}^2\right)\right]$$

The μ_e is also estimated by means of E_N^T using the below

$$(\bar{\nu}_a - \bar{\nu}_f) = 11307.6\left[\left(\frac{\Delta\mu}{\Delta\mu_s}\right)^2 \left(\frac{a_s}{a}\right)^3\right] E_N^T + \text{Constant}$$

Where $\Delta\mu_B$ is the change in dipole moment

a_S is the Onsager radius of the solvent

$\Delta\mu$ and a are the corresponding parameters of the compound [29].

9. HOMO and LUMO of 4MPPC

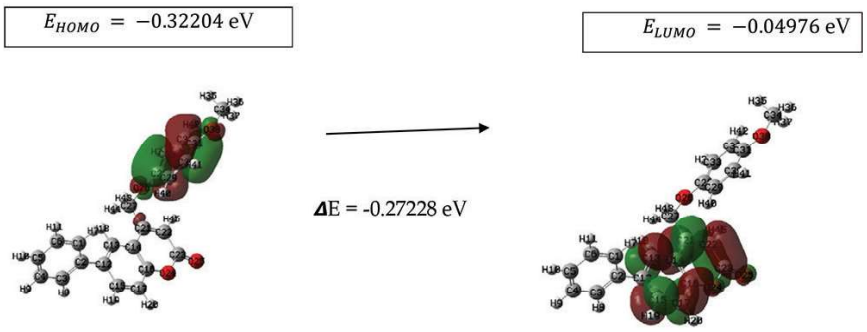

Figure 8: HOMO and LUMO of 4MPPC

10. Mulliken Charges

Mulliken Charges and Chemical Reactivity

Electron-rich (nucleophilic) centres: Oxygens (−0.3679 to −0.4471), carbons like C6, C12, C22.Electron-poor (electrophilic) centres: C23 (+0.6372), C16 (+0.2755), C31 (+0.2181). Strong intramolecular charge transfer (ICT) axis, especially across C23 and adjacent Oxygens, governs absorption/emission shifts [30]. This charge polarization boosts solvatochromic fluorescence and targets for reactivity or coordination [30-31].

Table 1: Mulliken charges of 4MPPC

1	**1C**	-0.166318	**16**	**16C**	0.275590	**31**	**31C**	0.218166
2	**2C**	0.025081	**17**	**17C**	-0.194183	**32**	**32C**	-0.197305
3	**3C**	-0.173991	**18**	**18H**	0.170937	**33**	**33C**	-0.196414
4	**4C**	-0.120805	**19**	**19H**	0.156613	**34**	**34C**	-0.189105
5	**5C**	-0.150161	**20**	**20H**	0.175212	**35**	**35H**	0.129435
6	**6C**	-0.119310	**21**	**21C**	0.089796	**36**	**36H**	0.155540
7	**7H**	0.145568	**22**	**22C**	-0.445558	**37**	**37H**	0.129846
8	**8H**	0.152438	**23**	**23C**	0.637218	**38**	**38O**	-0.388242
9	**9H**	0.145380	**24**	**24O**	-0.367949	**39**	**39H**	0.170492
10	**1H**	0.146480	**25**	**25O**	-0.447181	**40**	**40H**	0.175151
11	**1H**	0.144390	**26**	**26O**	-0.323972	**41**	**41H**	0.164120
12	**12C**	-0.026952	**27**	**27C**	-0.285909	**42**	**42H**	0.171802
13	**13C**	-0.105289	**28**	**28C**	0.157570	**43**	**43H**	0.303736
14	**14C**	-0.169349	**29**	**29C**	-0.200801	**44**	**44H**	0.262227
15	**15C**	-0.085132	**30**	**30C**	-0.150347	**45**	**45H**	0.201483

Table 2: Calculated values for solvent polarity parameters, λ_a, v_a and $\bar{\nu}_a$.

Absorption				
SL	**Solvents**	λ_a**(nm)**	v_a	$\bar{\nu}_a$
1	Propanol	296	1013513	33783
2	Butanol	226	1327433	44247
3	Heptanol	292	1027397	34246
4	Decanal	231	1298701	43290
5	Pentanol	220	1363636	45454
6	Toluene	290	1034482	34482
7	DMSO	281	1067615	35587
8	Benzene	286	1048951	34965
9	THF	262	1145038	38167
10	DMF	289	1038062	34602

Table 3: Calculated values for solvent polarity parameters, λ_f, v_f and $\bar{\nu}_f$.

Emission				
SL	**Solvents**	λ_f **(nm)**	v_f	$\bar{\nu}_f$
1	Propanol	299	1003344	33444
2	Butanol	324	925925	30864
3	Heptanol	359	835654	27855
4	Decanal	347	864553	28818
5	Pentanol	300	1000000	33333
6	Toluene	294	1020408	34013
7	DMSO	344	872093	29069
8	Benzene	295	1016949	33898
9	THF	319	940438	31347
10	DMF	284	1056338	35211

Table 4: Calculated values for solvent polarity parameters, $\bar{\nu}_a - \bar{\nu}_f$ $f_1(\varepsilon, n)$ **and** m_1

SL	**Solvents**	$\bar{\nu}_a - \bar{\nu}_f$	$f_1(\varepsilon, n)$	m_1
1	Propanol	10169	0.2746	37032
2	Butanol	401508	0.2633	1524906
3	Heptanol	191743	0.2525	929456
4	Decanal	434148	0.2041	2127133
5	Pentanol	363636	0.2524	1440713
6	Toluene	14074	0.3351	41999
7	DMSO	195522	0.2684	728472
8	Benzene	32002	0.0475	673726
9	THF	204600	0.1971	1038051
10	DMF	18276	0.2753	66385

Table 5: Calculated values for solvent polarity parameters, $\bar{\nu}_a - \bar{\nu}_f$, $f_2(\varepsilon, n)$ **and** m_2

SL	Solvents	$\bar{\nu}_a - \bar{\nu}_f$	$f_2(\varepsilon, n)$	m_2
1	Propanol	10168	0.524	19406
2	Butanol	401508	0.79	1524906
3	Heptanal	191743	0.652	929456
4	Decanal	434148	0.553	2127133
5	Pentanol	363636	0.716	1440713
6	Toluene	14074	0.142	41999
7	DMSO	195522	0.841	728472
8	Benzene	32002	0.475	673726
9	THF	204600	0.197	1038051
10	DMF	18276	0.839	66385

Table 6: Calculated values for solvent polarity parameters, $\boldsymbol{\nu}_a - \boldsymbol{\nu}_f$, f_2 (ε, n) +2g(n) and m_3

SL	Solvents	$\boldsymbol{\nu}_a - \boldsymbol{\nu}_f$	f_2 (ε, n) +2g(n)	m_3
1	Propanol	10168	1.305	7792
2	Butanol	401508	1.291	311005
3	Heptanal	191743	1.227	156269
4	Decanal	434148	1.146	378837
5	Pentanol	363636	1.273	285652
6	Toluene	14074	0.812	17332
7	DMSO	195522	1.489	131310
8	Benzene	32002	0.925	34596
9	THF	204600	0.749	273164
10	DMF	18276	1.422	12852

Table 7: Calculated values for solvent polarity parameters, $f_2(\varepsilon, n)$, g(n), $f_2(\varepsilon, n)$ + 2g(n)and $\frac{\lambda_a - \lambda_f}{f_2(\varepsilon,n) + 2g(n)}$

SL	Solvents	f_2 (ε, n)	**2g(n)**	f_2 (ε, n) +2g(n)	$\frac{\boldsymbol{\lambda_a - \lambda_f}}{\boldsymbol{f_2(\varepsilon, n) + 2g(n)}}$
1	propanol	0.781	0.524	1.305	2.29
2	Butanol	0.749	0.542	1.291	75.91
3	Heptanal	0.652	0.575	1.227	54.60
4	Decanol	0.553	0.593	1.146	101.22
5	Pentanol	0.716	0.557	1.273	62.84
6	Toluene	0.142	0.67	0.812	4.92
7	DMSO	0.841	0.648	1.489	42.31
8	Benzene	0.475	0.45	0.925	9.72
9	THF	0.197	0.552	0.749	76.10
10	DMF	0.839	0.583	1.422	3.51

Table 8: Calculated values for solvent polarity parameters, $\lambda_a - \lambda_f$, $\bar{\nu}_a - \bar{\nu}_f$, $\nu_a + \nu_f$, $\nu_a - \nu_f$, $\lambda_a + \lambda_f$, $\frac{\lambda_a + \lambda_f}{2}$ $\bar{\nu}_a + \bar{\nu}_f$ and $\frac{\bar{\nu}_a + \bar{\nu}_f}{2}$

SL	Solvents	$\lambda_a - \lambda_f$	$\bar{\nu}_a - \bar{\nu}_f$	$\nu_a + \nu_f$	$\nu_a - \nu_f$	$\lambda_a + \lambda_f$	$\frac{\lambda_a + \lambda_f}{2}$	$\bar{\nu}_a + \bar{\nu}_f$	$\frac{\bar{\nu}_a + \bar{\nu}_f}{2}$
1	Propanol	3	339	2016857	10169	595	297.5	6722859	3361429
2	Butanol	98	13383	2253358	401508	550	275	7511198	3755599
3	Heptanol	67	6391	1863051	191743	651	325.5	6210172	3105086
4	Decanal	116	14472	2163254	434148	578	289	7210848	3605424
5	Pentanol	80	12121	2363636	363636	520	260	7878787	3939393
6	Toluene	4	469	2054890	14074	584	292	6849636	3424818
7	DMSO	63	6518	1939708	195522	625	312.5	6465695	3232847
8	Benzene	9	1067	2065900	32002	581	290.5	6886334	3443167
9	THF	57	6820	2085476	204600	581	290.5	6951590	3475795
10	DMF	5	609	2094400	18276	573	286.5	6981334	3490667

Table 9: Calculated values for solvent polarity parameters, $f_1(\varepsilon,n)$, g(n), $f_1(\varepsilon, n)$ +g(n) and $\frac{\lambda_a - \lambda_f}{f_1(\varepsilon,n) + g(n)}$

SL	Solvents	$f_1(\varepsilon, n)$	g(n)	$f_2(\varepsilon, n) + g(n)$	$\frac{\lambda_a - \lambda_f}{f_1(\varepsilon,n) + g(n)}$
1	Propanol	0.2746	0.262	0.54	5.59
2	Butanol	0.2633	0.271	0.53	183.41
3	Heptanal	0.2525	0.285	0.54	124.65
4	Decanal	0.2041	0.296	0.50	231.95
5	Pentanol	0.2524	0.278	0.53	150.83
6	Toluene	0.3351	0.477	0.48	8.38
7	DMSO	0.2684	0.324	0.59	106.35
8	Benzene	0.0475	0.225	0.27	33.03
9	THF	0.1971	0.276	0.47	120.48
10	DMF	0.2753	0.291	0.57	8.829

Table 10: Some physical constants of solvents and absorption maxima of 4MPPC

SL	Solvents	n^a	ε^a	π^{*a}	m	β^a	λ_{max} (nm)
1	Propanol	1.385	20.6	0.52	0.8	0.9	296.92
2	Butanol	1.399	17.4	0.47	0.8	0.84	292.71
3	Heptanal	1.424	11.3	0.4	0.8	0.86	289.93
4	Decanal	1.41	14.8	0.4	0.8	0.86	291.24
5	Pentanol	1.437	8.0	0.45	0.7	0.82	220.32
6	Toluene	1.496	2.4	0.38	0.84	0.89	290.61
7	DMSO	1.479	47.24	1.0	0.65	0.76	281.44
8	Benzene	1.5	2.28	0.62	0.82	0.72	288.50
9	THF	1.406	7.4	0,73	0.75	0.75	292.71
10	DMF	1.43	38.25	0.88	0.76	0.69	287.08

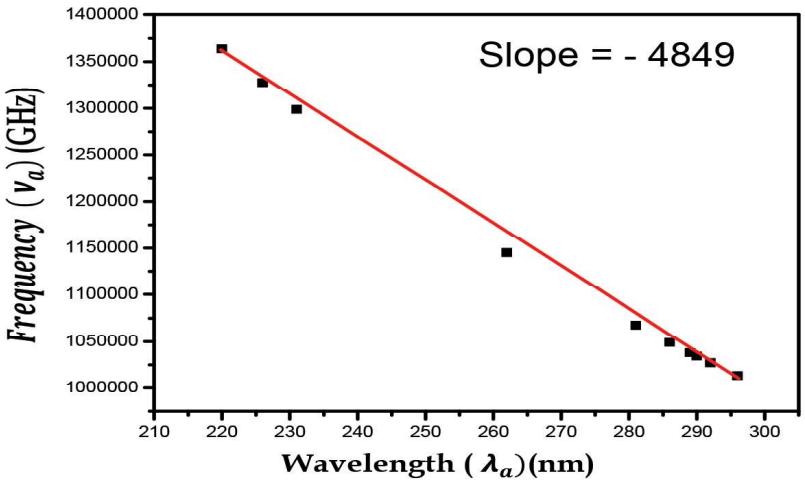

Figure 9: Absorption frequency Vs Absorption wavelength of 4MPPC

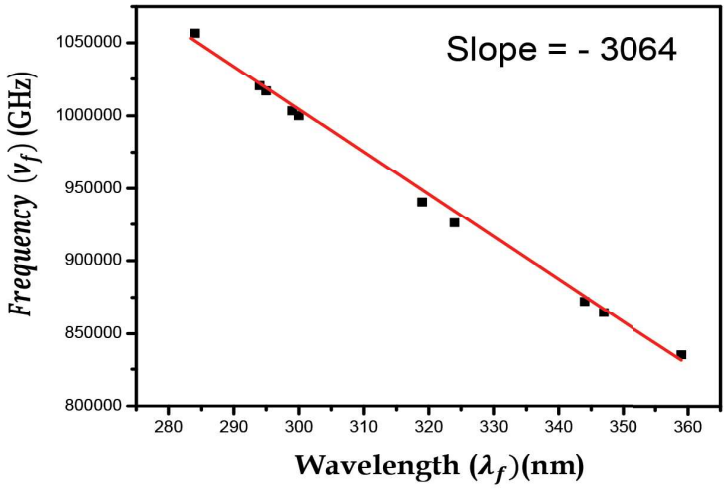

Figure 10: Fluorescence frequency Vs Fluorescence wavelength of 4MPPC

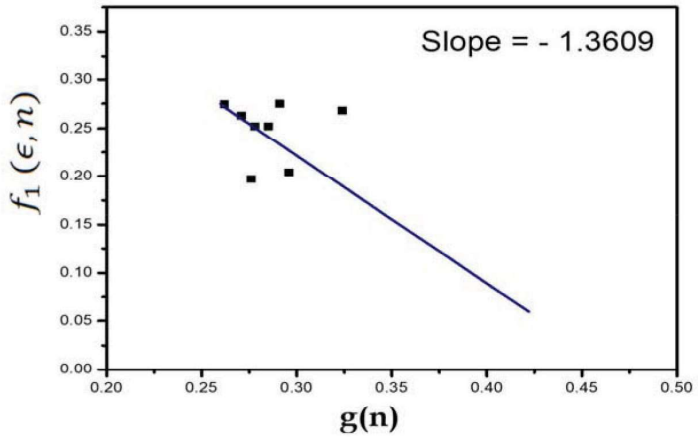

Figure 11: Lippert's graph, the variation of Orientation polarizability (f_1 (ε, n)) with Refractive index function g(n) of 4MPPC

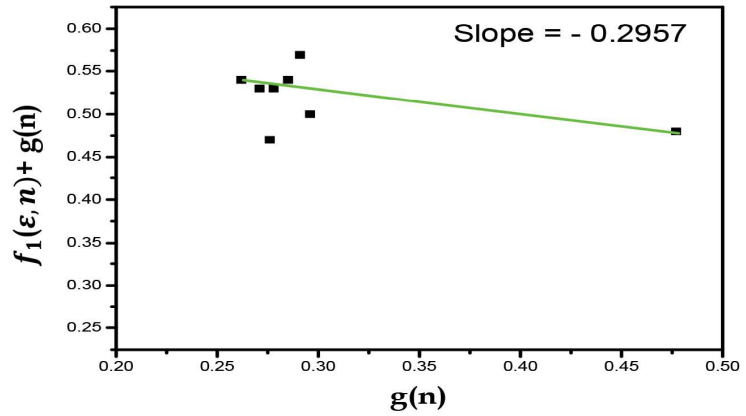

Figure 12: Dielectric–Refractive index correlation graph of 4MPPC, (f_1 (ε, n) + g(n) Vs g(n),

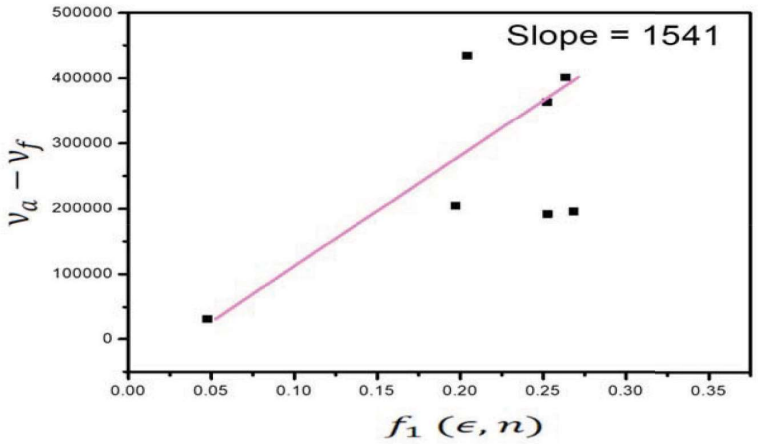

Figure 13: Lippert's polarity function, $\boldsymbol{\nu_a - \nu_f}$ Vs f_1 (ε,, n) of 4MPPC

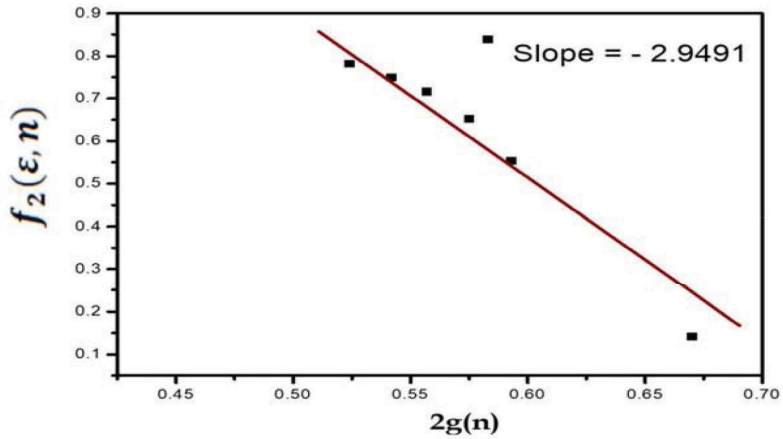

Figure 14: Bakshiev's polarity function of 4MPPC, (f_2 (ε, n)) Vs 2g(n)

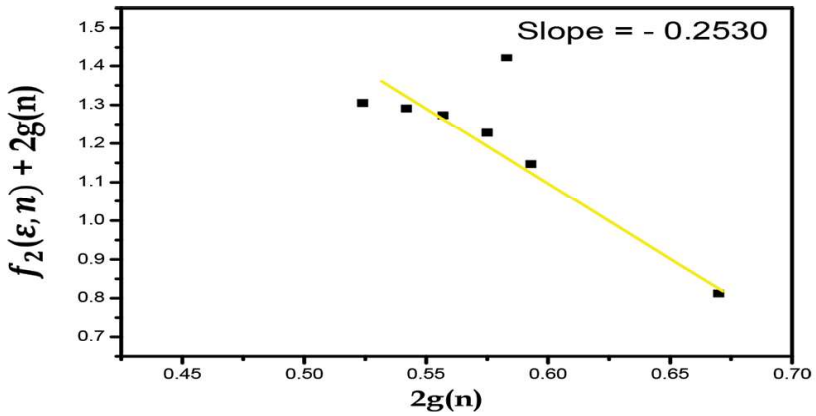

Figure 15: (f_2 (ε, n) + 2g(n) Vs 2g(n), Dielectric – Refractive index correlation graph of 4MPPC

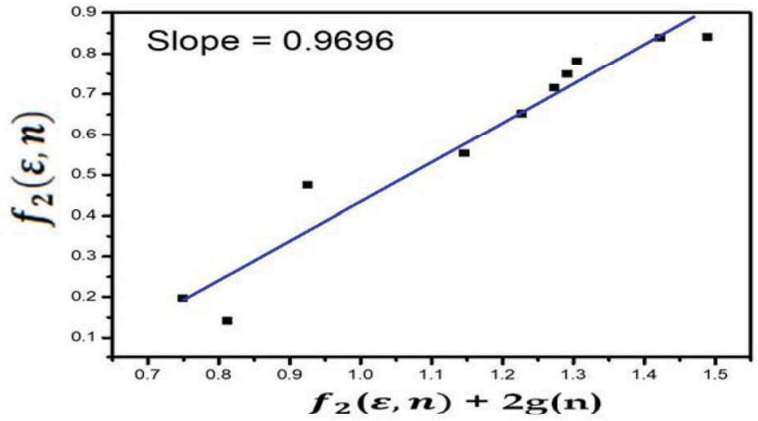

Figure 16: Bakshiev's polarity function of 4MPPC, (f_2 (ε, n) + Vsf_2 (ε, n) + 2g(n)

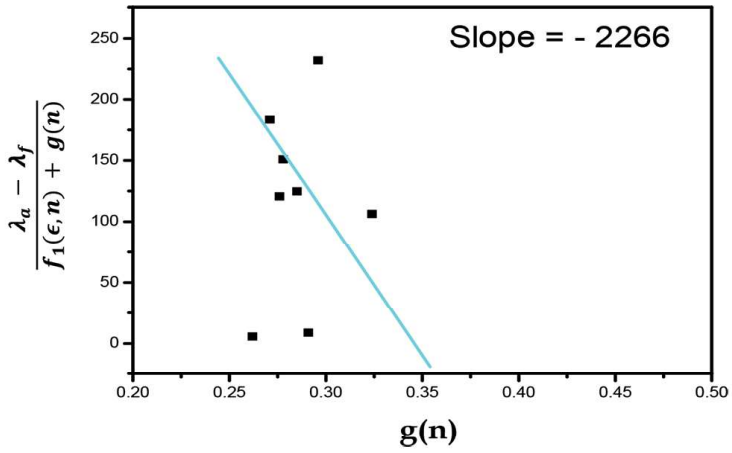

Figure 17: Lippert-Mataga graph of 4MPPPC, $\frac{\lambda_a - \lambda_f}{f_1(\varepsilon,n) + g(n)}$ Vs g(n)

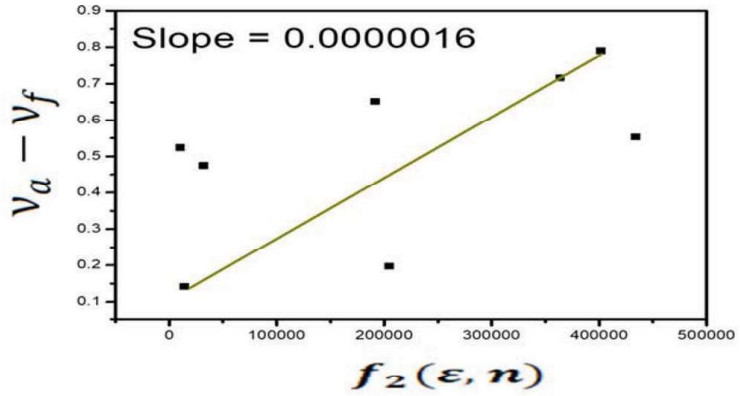

Figure 18: Bakshiev's polarity function of 4MPPC, $\boldsymbol{\nu_a - \nu_f}$ Vsf_2 (ε, n)

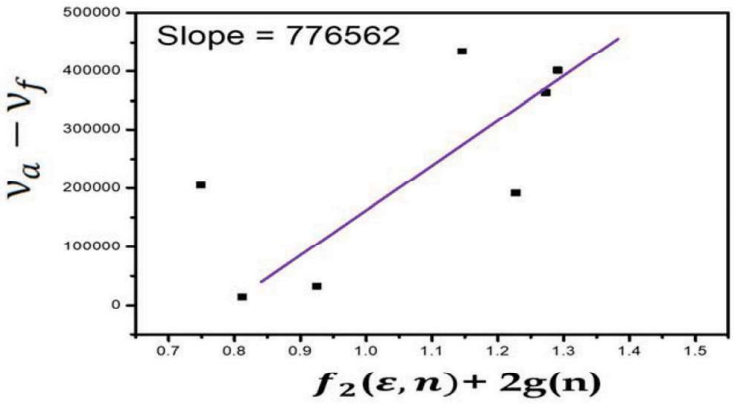

Figure 19: Bakshiev's polarity function of 4MPPC, $\boldsymbol{\nu_a - \nu_f}$ Vsf_2 (ε, n) + 2g(n)

11. Spectroscopic Features: UV-VIS Electronic Transitions

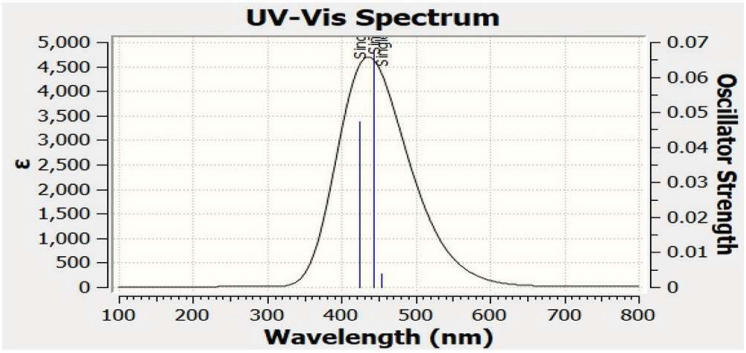

Figure 20: UV- VIS Spectrum of the molecule 4MPPC

Table 11: Excited states of 4MPPC

State	Energy(eV)	Wavelength (nm)	Oscillator Strength (f)	Assignment
Excited State 1(S_1)	2.7332	253.65	0.0037	HOMO→LUMO (sym forbidden)
Excited State 2(S_2)	2.7966	443.33	0.0676	HOMO-2/1→LUMO (π–π*)
Excited State 3(S_3)	2.9196	424.66	0.0473	Dominant UV absorption

Strong absorption at 424.66–443.33 nm (S_2/S_3) dominates UV-Vis spectrum [31-32]. Emission is expected from S_1, but with low quantum yield due to forbidden nature.

12. IR Vibrational Assignments

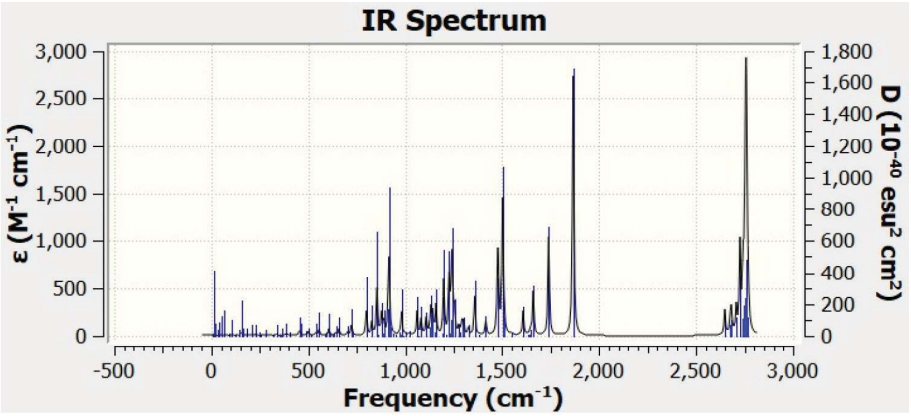

Figure 21: IR Spectrum of the molecule 4MPPC

C=O (Lactone): 1815, 1725 cm^{-1} (conjugation shifts the lower peak) [32]. Aromatic C=C: 1654, 1509 cm^{-1}.C–O–C (Ether/Methoxy): 1202–1243, 1049 cm^{-1} (strong fingerprint) [32-33].Aromatic C–H Stretch: 2650–2770 cm^{-1} (some peaks possibly overtones)Aromatic out-of-plane C–H bends: 810, 851, 910 cm^{-1} (indicative substitution patterns)No OH broad band: Consistent with structure. Spectra confirm the presence of a coumarin core, methoxy/ phenoxy substituents, and enhanced conjugation [33]

13. Dipole Moment and Polarizability (NLO Potential)

- Ground-state dipole: 7.3195 D (strong, anisotropic; dominates along X-axis).
- Isotropic polarizability (αiso): 2351 au (~34.85×10^{-24} cm^3) [33].
- First hyperpolarizability (βtot): ~5799 au (strong NLO response; Z-axis dominant).

High polarizability and hyperpolarizability make this chromophore a candidate for NLO applications (frequency doubling, electro-optic modulation) [34].

14. Key Checklists for Characterization

UV–Vis (in multiple solvents): Map solvatochromic shifts and molar absorptivity (ε) [34]. PL spectra + quantum yield: Compare to standards (quinine sulphate) or using an integrating sphere [35-36]. Time-resolved PL (τ, k, nr): Measure excited-state lifetimes [35].NMR (^{1}H, ^{13}C): Confirm assignable methoxy/phenoxy signals and aromatic patterns [36]. HRMS: Verify calculated mass and main fragments. Photobleaching test: Assess photostability under continuous illumination.

Table 12: Peak Assignments

Region (cm^{-1})	Approx. Peaks	Functional Group	Structural Motif
2640–2780	2650–2770	C–H stretching	Aliphatic/aromatic hydrogens
1500–1825	1509,1654,1725, 1815	C=C & C=O stretching	Conjugated aromatic and carbonyls
1202–1243	1202–1243	C–O, ring modes	Aryloxy methoxy, methoxy, aryl ethers
1049	1049	C–O stretch	Methoxy/phenoxy substituent
810–910	810, 851, 910	C–H (loop) bending	Substituted benzene/aryl rings

Table 13: Wavelength, Intensity of 4MPPC

Wavelength (nm)	Intensity (ε, $M^{-1}cm^{-1}$)	Assignment	Structural Origin
1815, 1725	Strong, very strong	C=O stretch (lactone/ ester)	Chromen-2-one coumarin carbonyl
1654,1509	Moderate/strong	Aromatic C=C stretch	Phenyl/coumarin aromatic rings
1202–1243	Strong cluster	C–O–C stretch, C–O, ring modes	Methoxy, phenoxy, aryl ethers, in-plane C–H bends
1049	Very strong	Alkyl/aryl C–O stretch	Phenoxy, methoxy ether group
810,851, 910	Strong	Aromatic C–H bend (loop)	Substituted aromatic environments
2650–2770	Multiple, moderate	Aliphatic/aromatic C–H stretches	Methoxy/benzylic/ aromatic hydrogens

Table 14: Comparative Table of Photophysical Feature Reference

Property	Definition	Significance/Usage
Absorption/ Emission	Wavelengths for photon absorption/emission	Indicates chromophore applications (imaging, optoelectronics)

Quantum Yield (Φ_f)	Emitted/absorbed photon ratio	High Φ_f = stronger fluorescence, better detection
Lifetime (τ_f)	Excited state residence time	Gives info on local environment, quenching, and FRET capability
Stokes Shift	Abs–Em peak separation	Minimizes reabsorption, enables clear spectral detection
Solvatochromism	Spectral shift with solvent polarity	Used for microenvironment sensors; environment-sensitive imaging
Photostability	Resistance to photobleaching	Required for long-duration fluorescence imaging
Dipole/ Polarizability	Molecular polarity and electron cloud distortion	Key for NLO materials, sensor/ bioelectronic interfaces
Charge Distribution	Mulliken atomic charges	Highlights donor–acceptor regions, guides functionalization/ development

15. Applications

- Fluorescent probes/dyes: Blue-green emitter with microenvironment sensitivity.
- Optoelectronics (OPV/OLED): Extended π-system, strong photostability, NLO activity [37].
- Sensors: FRET donor capability, ratio metric sensors tunable by substituent modification.
- Bioimaging: Stable fluorescence, solvatochromic response, low toxicity.

The IR spectrum features several **diagnostic bands** related to functional groups present in the coumarin-based molecule [37].

16. Molecular Structure and Evidence

Lactone carbonyl:

Strong doublets around **1725 cm^{-1}** (very strong, conjugated C=O) and **1815 cm^{-1}** (lactone C=O) [38]. Indicates coumarin-type core; lower C=O due to aromatic conjugation.

Aryl and ether motifs:

Intense features from **1202–1243 cm^{-1}** and **1049 cm^{-1}** validate multiple **phenoxy/methoxy substituents**.

Aromatic substitution:

Several strong out-of-plane modes (810–910 cm^{-1}) reveal various aromatic substitution environments.

Aliphatic/aromatic C–H stretches:

Multiple sharp signals at **2640–2780 cm^{-1}** fit the expected methoxy/benzylic hydrogens, though the region appears shifted low, as noted in the data comments [38].

Fingerprint region:

Rich, complex, indicative of multiple ring systems and ether linkages.

Recommended Checks:

Compare experimental spectrum with DFT-computed IR: Use a scaling factor (≈0.96–0.99) to match peak assignments to normal modes for confirmation.

Additional spectra (e.g., Raman, isotope labelling): Can help refine assignments of C–H, C–O, and aromatic vibrations [39].

17. Results from Computation

In the present investigation, the photophysical properties of the molecule is studied by using the computational methods. Firstly B3LYP/6-31 1+G (d, p) method is used to obtained the optimized ground state geometry. Using the TD- B3LYP/6-31 1+G (d, p) method, the ground state and excited state dipole moments, absorption and emission maxima in nm and HOMO-LUMO gap in eV to be calculated.

The theoretical photophysical properties of solute is in satisfactory agreement with the obtained experimentally findings with negligible error which is quite expectable due to inherent limitations of computational calculations.

The DFT studies on coumarin 4MPPC can provide valuable insights into its electronic structure and photophysical properties. It gives an idea about the Prediction of its reactivity and interactions with biomolecules, development of new coumarin derivatives with improved performance.

18. Future Scope

The study on coumarin 4MPPC can be extended to explore its potential in optoelectronics, such as OLEDs and sensors. It can be used to design and synthesize derivatives with improved properties. Its biological activity

and pharmaceutical applications can be probed. Advanced computational methods, like TD-DFT, can be used to further understand its photophysical properties. The study can also be extended to investigate its interactions with nanoparticles and biomolecules. This study can serve as a foundation for future research on coumarin-based compounds, exploring their potential in various fields.

19. Summary

The fluorescent molecule 4-(4-Methoxy-Phenoxymethyl)-6-phenyl-chromen-2-one (**4MPPC)** offers a rich conjugated framework that endows it with distinctive photophysical and nonlinear optical properties [39]. Its strong absorption and tenable emission, environment-sensitive behaviour, and pronounced IR fingerprints are tied to the extended aromaticity and functional group diversity. The charge distribution, dipole, and hyperpolarizability underline its capacity for nonlinear optics and sensing, while practical characterization is supported by IR/NMR/UV–Vis spectral features. Its robust fluorescence, polarizability, and photostability position it for diverse use in advanced imaging, sensing, and optoelectronic applications [40].

20. Conclusions

The ground and excited state dipole moments of coumarin (4MPPC) were evaluated based on its spectroscopic properties, which were influenced by solvent polarity [40-41]. Solvent effects on excitation and emission spectra were analyzed using various solvent polarity correlation methods. The ground state dipole moment was computationally estimated using Gaussian 16W software with B3LYP/6-31G basis set. Lippert-Mataga and Bakhshiev's methods were employed to determine the experimental excited state dipole moment of coumarin **(4MPPC)** [41-42].

21. Authorship contribution statement

Alageri Lingappa: Performed Experimental part and prepared manuscript. **Shivaleela B, Srinath and K. Narasimhalu:** Contributed valuable discussion to the data preparation, **J. Thipperudrappa:** Synthesis of title coumarin organic molecule, **S.M. Hanagodimath:** Corrected the experimental part and manuscript.

22. Declaration of competing interest

The author declare that they have no known competing financial interests or personal relationships that could have appeared to influence the reported in this paper.

23. Funding

The authors have no major funding from any scientific agency.

24. Author's statement

I sincerely thank the Editor and Reviewers of the journal for suggestions and constructive comments that helped us in upgrading the quality of the manuscript and also my research work. Please accept and publish our paper in your esteemed journal.

25. Section snippets: Reagents and apparatus

Spectroscopic-grade chemicals and solvents were obtained from Sigma-Aldrich and S.D. Fine Chemicals Ltd., India. Absorption and fluorescence spectra were recorded at room temperature using a UV–visible spectrophotometer at USIC, Gulbarga University and a spectrofluorophotometer at USIC, Karnataka University, respectively. Sample solutions (10^{-5} M) were prepared in solvents with varying polarities to minimize self-absorption.

26. Acknowledgement

We thank the Director and technical staff, USIC, Gulbarga University, Kalaburagi, for providing the Spectro fluorophotometer, Director and technical staff, USIC, Karnataka University, Dharwad, for providing the Spectro fluorophotometer.

References

[1]. S. Chandrasekhar, H.R. Deepa, R.M. Melavanki, S. Mogurampelly, M.M. Basanagouda, J.Thipperudrappa, S. Yallappa, Chem. Data Collect.29(2020),100516.

[2]. S. Chandrasekhar, H.R. Deepa, R. Melavanki, M.M. Basanagouda, S. Mogurampelly, J. Thipperudrappa, Luminescence.36(2021)769–787

[3]. Prajakta S. Kadolkar, Shivaraj A. Patil, Wari, Sanjeev R. Inamdar j.molliq.2020.113452.pdf

[4]. N.N. Hamdi, M.M. Chebli, H. Grib, M. Brahimi, A.M.S. Silva, Synthesis DFT/ TD- DFT theoretical studies and experimental solvatochromic shift methods on determination of ground and excited state dipole moments of 3-(2-hydroxybenzoyl) coumarins, J. Mol. Struct. 1175 (2019) 811–820, https://doi.org/ 10.1016/j.molstruc.2018.08.039.

[5]. L.C. Luz, M.G. Gündüz, R. Beal, G.M. Zanotto, E.R. Kuhn, P.A. Netz, C. S¸ afak, P.F.B. Gonçalves, Fabiano da silveira santos, fabiano severo rodembusch, J Photochem. Photobiol. 429 (2022), 113915.

[6]. Asnaashari M, Kenari RE, Taghdisi SM, Abnous K, Farahman dfar R (2024) A novel fluorescent DNA sensor for acrylamide detection in food samples based on Single-Stranded DNA and gelred. J Fluoresc 34:2845–2860, https://doi.org/ 10.1007/s10895-023-03479-7.

[7]. Erdemir GY, Topkaya D (2024) Synthesis, characterization and evaluating photochemical properties of Porphyrin-substituted Azobenzene structure. J Fluoresc 34:275–281. https://doi.org/10.1007/s10895-023-03256-6.

[8]. Essam ZM, Ozmen GE, Setiawan D, Hamid RR, Abd El-Aal RM, Aneja R, Hamelberg D, Henary M (2021) Donor acceptor fluorophores: synthesis, optical properties, TD-DFT and cytotoxicity studies. Org Biomol Chem 19:1835–1846. https://doi.org/10.1039/d0ob02313b

[9]. H.R. Deepa, S. Chandrasekhar, J. Thipperudrappa, Chem. Phys. Im pact4(2022), 100075.

[10]. Poronik YM, Baryshnikov GV, Deperasinska I, Espinoza EM, Clark JA, Ågren H, Gryko DT, Vullev VI (2020) Deciphering the unusual fluorescence in weakly coupled bis-nitro-pyrrolo[3,2-] pyrroles. Communications Chemistry 3. https://doi.org/ARTN.19010.1038/s42004-020-00434-6

[11]. Jing Han W, Chih-Ling C, Zhe Wei Z, Mahdy EL, Ahmed FM (2022) Facile metal-free synthesis of pyrrolo[3,2-b]pyrrolyl based conjugated microporous polymers for high- performance photocatalytic degradation of organic pollutants. Polym Chem 13:37:5300–5308.https://doi.org/10.1039 / d2py00658h

[12]. Bhardwaj K, Anand T, Jangir R, Sahoo SK (2024) Aggregation Induced emission active Benzidine-Pyridoxal derived scaffold for detecting Fe(3+) and pH. J Fluoresc 34:2917–2926. https://doi.org/10.1007/s10895-023-03503-w.

[13]. HA.Z. Sabek, AM.M. Alazaly, D. Salah, HS. Abdel-Samad, MA. Ismail, AA. Abdel- Shafi, RSC Adv. 10 (2020) 43459–43471.

[14]. S.N. Saravanamoorthy, G. Sathiyapriya, M. Sivasakthi, Int. J. Res. Appl. Sci. Eng. Technol. 7 (2019) 1017–1028 (IJRASET).

[15]. Mahesh, S. Najare , Mallikarjun K. Patil, Afra Quasar A. Nadaf , Shivaraj Mantur, Manjunatha Garbhagudi, Supreet Gaonkar , Sanjeev R. Inamdar , Imtiyaz Ahmed M. Khazi j.molstruc.2019.127032.pdf

[16]. Mallikarjun, K. Patil, M.G. Kotresh, Sanjeev R. Inamdar, https://doi.org/ 10.1016/j.saa.2019.02.022

[17]. Shivaraj A. Patil, Prajakta S. Kadolkar, Manjunath, N. Wari, Sanjeev, R. Inamdar, S2352492821007248.pdf

[18]. J. Thipperudrappa, D.S. Biradar, M.T. Lagare, S.M. Hanagodimath, S.R. Inmdar, J.S. Kadadevaramath,https://www.sciencedirect.com/science/ article/abs/pii/S1010603005002753? via%3Dihub

[19]. J. Thipperudrappa, D.S. Biradar, S.R. Manohara, S.M. Hanagodimath, S.R. Inamadar, R.J.Manekutla,https://www.sciencedirect.com/science/article/ abs/pii/S1386142507003186?via%3Dihub

[20]. M. K. Patil, M.G. Kotresh, S.R. Inamdar, Spectrochimica Acta Part A, DOI: S1386–1425(19)30134–9. https://doi.org/10.1016/j.saa.2019.02.022.

[21]. R.B. da Silva, F. Lange Coelho, F.S. Rodembusch, R.S. Schwab, J.M.F.M. Schneider,D. da Silveira Rampon, P.H. Schneider, New J. Chem. 43 (2019) 11596–11603.

[22]. Sanjeev, R. Inamdar, James, R. Mannekutla, M.S. Sannaikar, M.N. Wari, B.G. Mulimani, M.I. Savadatti, https://doi.org/10.1016/j.molliq.2018.07.005

[23]. G.H. Pujar, M.N. Wari, B. Steffi, H. Varsha, B. Kavita, C. Yohannan Panicker, http://dx.doi.org/10.1016/j.molliq.2017.08.078

[24]. Jana Basavaraja, S.R. Inamdar, H.M. Suresh Kumar j.saa.2016.07.010.pdf

[25]. S.K. Patila, M.N. Warib, C. Yohannan Panickerc, Inamdar, j.saa.2013.12.031.pdf

[26]. Airin Antony, J.Mitra, Refractive index-assisted UV/Vis spectrophoto metry to over come spectral interference by https://www.sciencedirect.com /science/article/abs/pii/S0003267020312691,

[27]. A. Frisch, R. Dennington, T. Keith, J. Millam, A. Nielsen, A.J. Holder, Hiscocks, Gauss View Version 5 User Manual, Gaussian Inc, Wallingford,CT,USA,2009.

[28]. N. Muruganantham, R. Sivakumar, N. Anbalagan, V.Gunasekaran, J. Thipperudrappa, Leonard,Biol. Pharm. Bull. 27 (2004) 1683–1687

[29]. Y.F. Nadaf, B.G. Mulimani, M. Gopal,. Inamdar, j.theochem.2004.01.049.pdf

[30]. S.P. Olivares, S.Risso, M.I. Gutie´rrez, Spectrochim. ActaA71(2008)336– 339

[31]. J.A. Dean, Lange'sHandbookofChemistry,15thed., McGraw-Hill, New York, 1999

[32]. X. Zhang, A.S. Shetty, S.A. Jenekhe, Macromolecules32(1999)7422–7429

[33]. J.R. Lackowicz, Principles of Fluorescence Spectroscopy, Plenum Press, New York,1983.z

[34]. M.J. Kamlet, J.L.M. Abboud, M.H. Abraham, R.W. Taft, J. Org. Chem. 48 (1983)2877–2887..

[35]. M.J. Kamlet, Prog. Phys.Org.Chem.13(1982)485.

[36]. M. J. Kamlet, J. L. Abboud, R.W.Taft, J.Am.Chem.Soc.99(1977)6027–6038

[37]. P.H. Vandewyer, J. Hoefnagels, G. Smets, Tetrahedron25(1969)3251–3266.

[38]. N. Mataga, Y. Kaifu, M. Koizumi, Bull. Chem. Soc.Jpn.29(1956)465–470

[39]. Hawks AM, Altman D, Faddis R, Wagner EM, Bell KJ, Charland Martin A, Collier GS (2023) Relating design and optoelectronic properties of 1,4-Dihydropyrrolo [3,2-b] pyrroles bearing biphenyl substituents. J Phys Chem B 127:7352–7360. https://doi.org/10.1021/acs.jpcb.3c03061.

[40]. Hawks AM, Daniel LM, Sorto VS, Mauro J, Skiouris P, Collier GS (2024) Expanding color control of anodically coloring electrochromes based on Electron-Rich 1,4-Dihydropyrrolo [3,2-b] pyrroles. ACS Appl Opt Mater 2:1235– 1244. https://doi.org/10.1021/acsaom.4c00197

[41]. Radha Goudar, Ritu Gupta, Giridhar U. Kulkarni, Sanjeev R. Inamdar, J. Fluoresc. 25(2015) 1671–1679, https://doi.org/10.1007/s10895-015-1654-6.

[42]. V.V. Koppal, Raveendra Melavanki, Raviraj Kusanur, N.R. Patil, Analysis of Fluorescence Quenching of Coumarin Derivative under Steady State and Transient State Methods, https://doi.org/10.1007/s10895-020-02663-3